Front. Optoelectron. China 2010, 3(4): 399–407
DOI 10.1007/s12200-010-0126-5

RESEARCH ARTICLE

Propagating property of flat-topped multi-Gaussian beams passing through a misaligned optical system with two-lens and two-diaphragm

Hongbin SHEN (✉)[1], Gang LI[1], Han ZHANG[2], Wengang HU[1], Bing ZHOU[1], Bingqi LIU[1]

1 Department of Optics and Electronic Engineering, Ordnance Engineering College, Shijiazhuang 050003, China
2 Department of Computer Engineering, Ordnance Engineering College, Shijiazhuang 050003, China

Abstract The optical elements' maladjustment is a potential threaten in optical systems, thus, the transmission feature of laser beams passing through a misaligned optical system is widely studied. By using approximate expansion of circle diaphragm and generalized Huygens-Fresnel diffraction formula, a universal analytic expression is deduced for the flat-topped multi-Gaussian beams passing through a misaligned optical system with two-lens and two-diaphragm. The study on the propagating property of fundamental-mode Gaussian beams and a flat-topped multi-Gaussian beam is carried out accordingly. The expansion of complex Gauss function of misaligned optical circle diaphragm is given, as well as a group of new parameter values of the expansion of complex Gauss function. By using the new parameter values, the influence of disadjust parameters on output intensity distribution is analyzed numerically. The result shows that the diaphragms' offset can make the beams offset or covered, and the second diaphragm influences more; the angle deflection of diaphragms can make light beams compressed in the deflection direction, and the first diaphragm influences more; the offset of the first lens can weaken light intensity in the same direction of the lens offset, and the offset of the second lens can weaken light intensity in the opposite direction of the lens offset; the angle deflection of the first lens can make light beams move to the opposite direction, and the angle deflection of the second lens has no influence; when all the diaphragms and the lenses are disadjust, the angle deflection of the first lens has a vital influence to the output intensity distribution.

Keywords laser optics, flat-topped multi-Gaussian beams, misaligned optical system, circle diaphragms

Received March 23, 2010; accepted October 12, 2010

E-mail: shenhongbin11@sina.com

1 Introduction

The propagation and transformation of laser passing through an optical system are restricted by optical elements in the system, such as diaphragm, lens, and so on. Many researchers [1–19] have studied and reported the propagating property of many kinds of Gaussian beams passing through paraxial *ABCD* optical system. The flat-topped Gaussian beams is one of the typical laser beam models, thus, its propagation properties have been widely studied, for example, the propagation factor, the kurtosis parameter, the focusing properties of flat-topped Gaussian beams, and the expressions for flat-topped Gaussian beams propagating through an apertured *ABCD* optical system have been derived. However, these studies applied only for normal optical system. As a matter of fact, there would be optical elements' misalignment such as diaphragms, so study on the universal analytic expression of laser passing through a misaligned optical system with lenses and diaphragms is of great importance. In this paper, the approximate analytic expression of flat-topped multi-Gaussian beams passing through an optical system with two-lens and two-diaphragm is deduced, and the propagating property of flat-topped multi-Gaussian beams passing through a normal and misaligned optical system with two-lens and two-diaphragm is studied based on this expression. Some samples have been taken to demonstrate the analysis process.

2 Theoretical analysis

Flat-topped multi-Gaussian beams can be simulated with coherent combination of off-axis multi-Gaussian beams. Figure 1 shows the sketch map of optical system with two-lens and two-diaphragm.

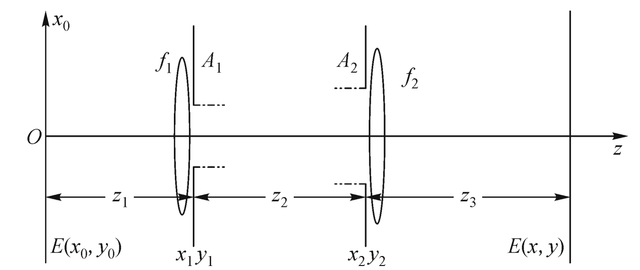

Fig. 1 Sketch map of optical system with two-lens and two-diaphragm

In Fig. 1, the input complex amplitude distribution of the optical system with two-diaphragm and two-lens is [5]

$$E(x_0,y_0) = E_0 \frac{\sum_{n=-N}^{N} \exp\left\{-\frac{(x_0-nw_0)^2}{w_0^2}\right\} \sum_{n=-N}^{N} \exp\left\{-\frac{(y_0-nw_0)^2}{w_0^2}\right\}}{\sum_{n=-N}^{N} \exp\{-n^2\} \sum_{n=-N}^{N} \exp\{-n^2\}}, \tag{1}$$

where w_0 is the waist radius of the fundamental-mode of Gaussian beams, N is the exponent number, and $2N+1$ is the superimposed Gaussian beams number. The connection between w_0 and the waist radius W of the flat-topped Gaussian beams is

$$w_0 = \frac{W}{N + \left\{1 - \ln\left[\sum_{n=-N}^{N} \exp\{-n^2\}\right]\right\}^{1/2}}. \tag{2}$$

When $N=0$, Eq. (1) is the field distribution of fundamental-mode Gaussian beams:

$$E(x_0,y_0) = E_0 \exp\left\{-\frac{x_0^2+y_0^2}{w_0^2}\right\}. \tag{3}$$

According to generalized diffraction formula, the output complex amplitude distribution of flat-topped multi-Gaussian beams passing through the misaligned optical system is

$$\begin{aligned} E(x_2,y_2) = {} & \frac{\mathrm{i}k}{2\pi B} \iint_S E_1(x_1,y_1) T(x_1,y_1) \\ & \cdot \exp\left\{-\frac{\mathrm{i}k}{2B}[A(x_1^2+y_1^2) - 2(x_1x_2+y_1y_2) \right. \\ & + D(x_2^2+y_2^2) + Ex_1 + Fy_1 + Gx_2 \\ & \left. + Hy_2]\right\} \mathrm{d}x_1 \mathrm{d}y_1, \end{aligned} \tag{4}$$

where A, B, C, and D are the matrix elements of normal optical system,

$$\begin{aligned} E &= 2(\alpha_T \varepsilon_x + \beta_T \varepsilon_x'), \\ F &= 2(\alpha_T \varepsilon_y + \beta_T \varepsilon_y'), \\ G &= 2(B\gamma_T - D\alpha_T)\varepsilon_x + 2(B\delta_T - D\beta_T)\varepsilon_x', \\ H &= 2(B\gamma_T - D\alpha_T)\varepsilon_y + 2(B\delta_T - D\beta_T)\varepsilon_y', \end{aligned}$$

where ε_x, ε_x' and ε_y, ε_y' are the position offsets and angle deflection in the x and y directions, respectively. The disadjust matrix elements are: $\alpha_T = 1-A$, $\beta_T = 1-B$, $\gamma_T = -C$, and $\delta_T = \pm 1 - D$. $E_1(x,y)$, $E_2(x,y)$ and $E(x,y)$ can be deduced from Eq. (4), and thus the output complex amplitude distribution is

$$\begin{aligned} E(x,y) = {} & \frac{\mathrm{i}k}{2\pi B_2} \iint_S \frac{\mathrm{i}k}{2\pi z_2} \iint_S \frac{\mathrm{i}k}{2\pi B_1} \iint_S E_0(x_0,y_0) \\ & \cdot \exp\left\{\frac{\mathrm{i}k}{2B_1}[A_1(x_0^2+y_0^2) - 2(x_0x_1+y_0y_1) + D_1(x_1^2+y_1^2) + E_1x_0 + F_1y_0 + G_1x_1 + H_1y_1]\right\} \mathrm{d}x_0 \mathrm{d}y_0 \\ & \cdot T_1(x_1,y_1) \exp\left\{\frac{\mathrm{i}k}{2z_2}[(x_2-x_1)^2 + (y_2-y_1)^2]\right\} \mathrm{d}x_1 \mathrm{d}y_1 \\ & \cdot T_2(x_2,y_2) \exp\left\{\frac{\mathrm{i}k}{2B_2}[A_2(x_1^2+y_1^2) - 2(x_1x_2+y_1y_2) + D_2(x_2^2+y_2^2) + E_2x_1 + F_2y_1 + G_2x_2 + H_2y_2]\right\} \mathrm{d}x_2 \mathrm{d}y_2, \end{aligned} \tag{5}$$

where A_1, B_1, C_1, and D_1 are the $ABCD$ matrix elements of normal optical system from primary plane to the back surface of the first lens; E_1, F_1, G_1, and H_1 are disadjust matrix elements in this transmission process; A_2, B_2, C_2, and D_2 are $ABCD$ matrix elements of normal optical system from the back surface of the second lens to observation plane, and E_2, F_2, G_2, and H_2 are the disadjust matrix elements in this transmission process.

The aperture function of the circle diaphragm is

$$T(x,y) = \begin{cases} 1, & \sqrt{(x-d_x)^2 + (y-d_y)^2} \leqslant r, \\ 0, & \sqrt{(x-d_x)^2 + (y-d_y)^2} > r, \end{cases} \tag{6}$$

where r is the diaphragm's radius, d_x and d_y are the deviations from axis z to the center of the diaphragm in the x and y directions, respectively.

When the diaphragm is disadjust, the expanded complex Gauss function formula is

$$T(x,y)=\sum_{m=1}^{M}F_m\exp\left\{-\frac{G_m[(r\cos\alpha_y)^2(x-d_x)^2+(r\cos\alpha_x)^2(y-d_y)^2]}{(r\cos\alpha_x)^2(r\cos\alpha_y)^2}\right\},\tag{7}$$

where α_x and α_y are the rake angle of diaphragm which are relative to axis z in the x and y directions, respectively, F_m and G_m are the expanded complex Gauss coefficients which are defined in Sect. 3. When $M=10$, the precision is enough if Eq. (7) is used to express Eq. (6).

Substitute Eqs. (1) and (7) into Eq. (5), the output complex amplitude distribution is

$$\begin{aligned}E(x,y)=&\frac{\mathrm{i}k}{2\pi B_2}\iint_S\frac{\mathrm{i}k}{2\pi z_2}\iint_S\frac{\mathrm{i}k}{2\pi B_1}\iint_S E_0\frac{\sum_{n=-N}^{N}\exp\left\{-\frac{(x_0-nw_0)^2}{w_0^2}\right\}\sum_{n=-N}^{N}\exp\left\{-\frac{(y_0-nw_0)^2}{w_0^2}\right\}}{\sum_{n=-N}^{N}\exp\{-n^2\}\sum_{n=-N}^{N}\exp\{-n^2\}}\\&\cdot\exp\left\{\frac{\mathrm{i}k}{2B_1}[A_1(x_0^2+y_0^2)-2(x_0x_1+y_0y_1)+D_1(x_1^2+y_1^2)+E_1x_0+F_1y_0+G_1x_1+H_1y_1]\right\}\mathrm{d}x_0\mathrm{d}y_0\\&\cdot\sum_{v=1}^{V}F_v\exp\left\{-\frac{G_v[(r\cos\alpha_y)^2(x-d_x)^2+(r\cos\alpha_x)^2(y-d_y)^2]}{(r\cos\alpha_x)^2(r\cos\alpha_y)^2}\right\}\\&\cdot\exp\left\{\frac{\mathrm{i}k}{2z_2}[(x_2-x_1)^2+(y_2-y_1)^2]\right\}\mathrm{d}x_1\mathrm{d}y_1\\&\cdot\sum_{u=1}^{U}F_u\exp\left\{-\frac{G_u[(r\cos\alpha_y)^2(x-d_x)^2+(r\cos\alpha_x)^2(y-d_y)^2]}{(r\cos\alpha_x)^2(r\cos\alpha_y)^2}\right\}\\&\cdot\exp\left\{\frac{\mathrm{i}k}{2B_2}[A_2(x_1^2+y_1^2)-2(x_1x_2+y_1y_2)+D_2(x_2^2+y_2^2)+E_2x_1+F_2y_1+G_2x_2+H_2y_2]\right\}\mathrm{d}x_2\mathrm{d}y_2.\end{aligned}\tag{8}$$

Two useful mathematical formulas are

$$\begin{aligned}&\iint_S E_1(x_1,y_1)\iint_S E_0(x_0,y_0)\mathrm{d}x_0\mathrm{d}y_0\mathrm{d}x_1\mathrm{d}y_1\\&=\iint_S\iint_S E_0(x_0,y_0)E_1(x_1,y_1)\mathrm{d}x_0\mathrm{d}y_0\mathrm{d}x_1\mathrm{d}y_1\\&=\iint_S\iint_S E_0(x_0,y_0)E_1(x_1,y_1)\mathrm{d}x_1\mathrm{d}y_1\mathrm{d}x_0\mathrm{d}y_0\\&=\iint_S E_0(x_0,y_0)\iint_S E_1(x_1,y_1)\mathrm{d}x_1\mathrm{d}y_1\mathrm{d}x_0\mathrm{d}y_0,\end{aligned}\tag{9}$$

$$\int_{-\infty}^{\infty}\exp(-w^2x^2\pm qx)\mathrm{d}x=\exp\left\{\frac{q^2}{4w^2}\right\}\frac{\sqrt{\pi}}{w},\quad \mathrm{Re}(w^2)>0\,.\tag{10}$$

Substitute Eqs. (9) and (10) to simplify Eq. (8), the analytical formula of $E(x,y)$ is deduced:

$$E(x,y)=\frac{E_0}{\mathrm{i}\lambda^3B_1B_2z_2}\exp\left\{\frac{\mathrm{i}k}{2B_2}[D_2(x^2+y^2)+G_2x+H_2y]\right\}$$
$$\cdot\sum_{v=1}^{V}F_v\frac{\pi}{w_{x1}w_{y1}}\exp\left\{-\frac{G_vd_{x1}^2}{(r_1\cos\alpha_{x1})^2}\right\}\exp\left\{-\frac{G_vd_{y1}^2}{(r_1\cos\alpha_{y1})^2}\right\}$$
$$\cdot\sum_{u=1}^{U}F_u\frac{\pi}{w_{x2}w_{y2}}\exp\left\{-\frac{G_ud_{x2}^2}{(r_2\cos\alpha_{x2})^2}\right\}\exp\left\{-\frac{G_ud_{y2}^2}{(r_2\cos\alpha_{y2})^2}\right\}$$
$$\cdot\exp\left\{\frac{M_{x2}^2}{4w_{x2}^2}+\frac{M_{y2}^2}{4w_{y2}^2}\right\}\exp\left\{-\frac{k^2}{4z_3^2}\left(\frac{x^2}{w_{x2}^2}+\frac{y^2}{w_{y2}^2}\right)\right\}\exp\left\{-\frac{\mathrm{i}k}{2z_3}\left(\frac{M_{x2}}{w_{x2}^2}x+\frac{M_{y2}}{w_{y2}^2}y\right)\right\}$$
$$\cdot\exp\left\{\frac{A_{x1}^2}{4w_{x1}^2}\right\}\exp\left\{\frac{A_{y1}^2}{4w_{y1}^2}\right\}\frac{\sum_{n=-N}^{N}\frac{\sqrt{\pi}}{w_{x0}}\exp\left\{\frac{q_{x0}^2}{4w_{x0}^2}\right\}\exp\{-n^2\}\sum_{n=-N}^{N}\frac{\sqrt{\pi}}{w_{y0}}\exp\left\{\frac{q_{y0}^2}{4w_{y0}^2}\right\}\exp\{-n^2\}}{\sum_{n=-N}^{N}\exp\{-n^2\}\sum_{n=-N}^{N}\exp\{-n^2\}},\tag{11}$$

where d_{x1} and α_{x1} are position offsets and angle deflection of the first diaphragm in the x direction, and d_{y1} and α_{y1} are position offsets and angle deflection of the first diaphragm in the y direction; d_{x2} and α_{x2} are position offsets and angle deflection of the second diaphragm in the x direction, and d_{y2} and α_{y2} are position offsets and angle deflection of the second diaphragm in the y direction. Other parameters are intermediate quantities in the deduction course, and they can be expressed as

$$A_1=1,\ B_1=z_1,\ C_1=-\frac{1}{f_1},\ D_1=1-\frac{z_1}{f_1},$$
$$E_1=0,\ F_1=0,$$
$$G_1=\frac{2z_1}{f_1}(\varepsilon_{x1}+z_1\varepsilon'_{x1}),\ H_1=\frac{2z_1}{f_1}(\varepsilon_{y1}+z_1\varepsilon'_{y1}),$$
$$A_2=1-\frac{z_3}{f_2},\ B_2=z_3,\ C_2=-\frac{1}{f_2},\ D_2=1,$$
$$E_2=\frac{2z_3}{f_2}\varepsilon_{x2},\ F_2=\frac{2z_3}{f_2}\varepsilon_{y2},\ G_2=0,\ H_2=0,$$
$$w_{x0}^2=\frac{k^2}{4z_1^2w_{x1}^2}+\frac{1}{w_0^2}-\frac{\mathrm{i}kA_1}{2B_1}-\frac{R_{x2}^2}{4w_{x2}^2},$$
$$q_{x0}=\frac{\mathrm{i}kE_1}{2B_1}+\frac{M_{x2}R_{x2}}{2w_{x2}^2}+\frac{2n}{w_0}-\frac{\mathrm{i}kA_{x1}}{2z_1w_{x1}^2}-\frac{\mathrm{i}kR_{x2}x}{2z_3w_{x2}^2},$$
$$w_{y0}^2=\frac{k^2}{4z_1^2w_{y1}^2}+\frac{1}{w_0^2}-\frac{\mathrm{i}kA_1}{2B_1}-\frac{R_{y2}^2}{4w_{y2}^2},$$
$$q_{y0}=\frac{\mathrm{i}kF_1}{2B_1}+\frac{M_{y2}R_{y2}}{2w_{y2}^2}+\frac{2n}{w_0}-\frac{\mathrm{i}kA_{y1}}{2z_1w_{y1}^2}-\frac{SR_{y2}y}{2w_{y2}^2},$$
$$w_{x1}^2=\frac{G_v}{(r_1\cos\alpha_{x1})^2}-\frac{\mathrm{i}kD_1}{2B_1}-\frac{\mathrm{i}k}{2z_2},$$
$$A_{x1}=\frac{2G_vd_{x1}}{(r_1\cos\alpha_{x1})^2}+\frac{\mathrm{i}kG_1}{2z_1},\ B=\frac{\mathrm{i}k}{z_2},\ C=\frac{\mathrm{i}k}{z_1},$$
$$w_{y1}^2=\frac{G_v}{(r_1\cos\alpha_{y1})^2}-\frac{\mathrm{i}kD_1}{2B_1}-\frac{\mathrm{i}k}{2z_2},$$
$$A_{y1}=\frac{2G_vd_{y1}}{(r_1\cos\alpha_{y1})^2}+\frac{\mathrm{i}kH_1}{2z_1},$$
$$w_{x2}^2=\frac{G_u}{(r_2\cos\alpha_{x2})^2}-\frac{B^2}{4w_{x1}^2}-\frac{\mathrm{i}k}{2z_2}-\frac{\mathrm{i}kA_2}{2B_2},$$
$$M_{x2}=\frac{2G_ud_{x2}}{(r_2\cos\alpha_{x2})^2}-\frac{\mathrm{i}kG_vd_{x1}}{z_2w_{x1}^2(r_1\cos\alpha_{x1})^2}+\frac{k^2G_1}{4z_1z_2w_{x1}^2}+\frac{\mathrm{i}kE_2}{2z_3},$$
$$R_{x2}=-\frac{k^2}{2z_1z_2w_{x1}^2},$$
$$S=\frac{\mathrm{i}k}{z_3},$$
$$w_{y2}^2=\frac{G_u}{(r_2\cos\alpha_{y2})^2}-\frac{B^2}{4w_{y1}^2}-\frac{\mathrm{i}k}{2z_2}-\frac{\mathrm{i}kA_2}{2B_2},$$
$$M_{y2}=\frac{2G_ud_{y2}}{(r_2\cos\alpha_{y2})^2}-\frac{\mathrm{i}kG_vd_{y1}}{z_2w_{y1}^2(r_1\cos\alpha_{y1})^2}+\frac{k^2H_1}{4z_1z_2w_{y1}^2}+\frac{\mathrm{i}kF_2}{2z_3},$$
$$R_{y2}=-\frac{k^2}{2z_1z_2w_{y1}^2},$$

where ε_{x1} and ε'_{x1} are the position offsets and angle deflection of the first lens in the x direction, and ε_{y1} and ε'_{y1} are position offsets and angle deflection of the first lens in the y direction; ε_{x2} is the offset of the second lens in the x direction, and ε_{y2} is the offset of the second lens in the y direction;

Equation (11) is the universal analytic expression that the flat-topped multi-Gaussian beams pass through the misaligned optical system. When $N=0$, it describes the fundamental-mode Gaussian beams. When every disadjust parameter is zero, it can be used to express the situation of normal optical system.

3 Optimization of F_m and G_m

F_m and G_m are complex constants, and they can be defined when the error variance of gate function, which is expressed by expanded complex Gauss function formula, is minimal. That is,

$$\begin{cases} \dfrac{\partial}{\partial F_k}\displaystyle\int_0^{\infty}\left[\mathrm{rect}(x)-\sum_{n=1}^{N}F_n\exp\{-G_n x^2\}\right]^2 \mathrm{d}x = 0, \\ \dfrac{\partial}{\partial G_k}\displaystyle\int_0^{\infty}\left[\mathrm{rect}(x)-\sum_{n=1}^{N}F_n\exp\{-G_n x^2\}\right]^2 \mathrm{d}x = 0, \end{cases} \quad k=1,2,\ldots,KN. \tag{12}$$

Reference [1] gives a group of parameter values when $N = 10$, and in Table 1 a group of parameter values that work out by Matlab optimization are given. Figure 2 plots the curves of real and imaginary parts of complex Gauss function and gate function curve of the diaphragm based on Ref. [1]. Figure 3 is the result based on this paper. Comparing Figs. 3 and 2, the advantage of the new parameters are: a) When $0<x<1$, the wave is flat, and its oscillation amplitude is smaller; b) When $0<x<2$, the curve of imaginary part is a line whose approximation is zero. This is because G_m in the new parameters appears in the form of conjugate complex couples, and F_m is also approximated to conjugate complpex.

4 Numeric analysis and discussion

Defining primary parameters: $z_1 = 150$ mm, $z_2 = 250$ mm, $r_1 = 1$ mm, $r_2 = 1$ mm, $f_1 = 100$ mm, $f_2 = 150$ mm, $w_0 = 1$ mm, $\lambda = 1.06$ μm, $N=5$, and calculate numerically by Matlab as below.

4.1 In normal situation

Figure 4 gives normalization intensity distribution in different propagating distances of flat-topped multi-Gaussian beams passing through the normal optical system. It shows that with the increment of diffraction distance, the beams diffuse, the top appears sunk, and the character of Gauss distribution appears gentle.

4.2 In situation of maladjustment

Equation (11) shows that x and y can exchange with each other in expression $E(x,y)$, thus the maladjustment in the x direction is just discussed in this paper. Planforms are adopted in order to observe the change of intensity distribution clearly that is created because of maladjustment. Figure 5, the planform of Fig. 4(b), is the intensity distribution of flat-topped multi-Gaussian beams passing through the system when $z_3 = 1000$ mm. In Fig. 6, intensity distribution of flat-topped multi-Gaussian beams passing through the system is given when just the diaphragm is

Table 1 Optimization value of F_m and G_m

F_m	G_m
0.07559598490 + 0.09012483874i	0.9287553876 + 12.99040532i
0.05330581361 + 0.1089269224i	0.9303989513 – 12.75022110i
– 0.6950302475 + 0.09507580544i	1.818923321 – 4.635611394i
0.7058623794 + 0.2364144607i	1.567848188 + 1.673830479i
0.6636344189 + 0.1859935477i	1.350921436 + 0.4065192793i
– 0.7558507154 – 0.4085011653i	2.046252095 + 4.847208786i
0.03729017757 – 0.1768490893i	1.092441026 – 2.492575124i
0.1408599406 + 0.3774909678i	1.687328598 + 8.824665168i
0.5223302799 – 0.0005666655990i	1.315310132 – 0.8774384876i
0.2341488018 – 0.3297827992i	1.668229170 – 8.579171116i

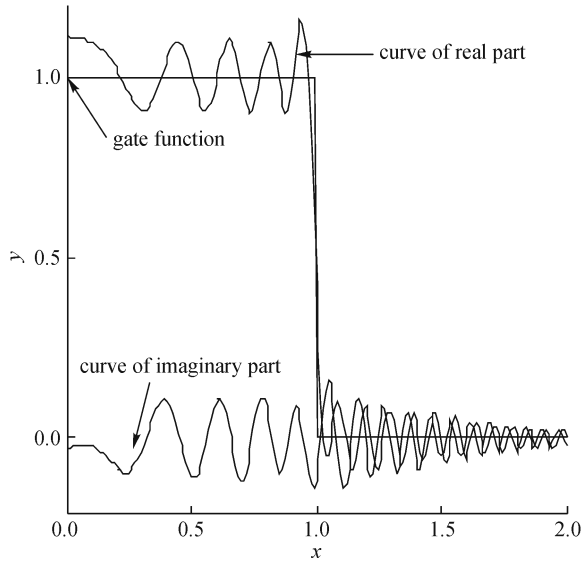

Fig. 2 Curves of real and imaginary parts of complex Gauss function based on Ref. [1]

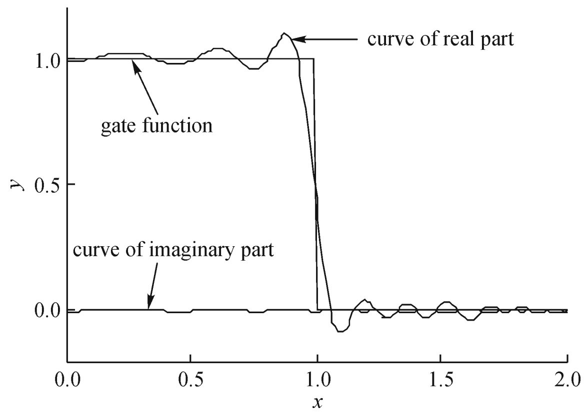

Fig. 3 Curves of real and imaginary parts of complex Gauss function based on this paper

disadjust. Figure 6(a) gives the situation when the position offset of the first diaphragm in the x direction (positive direction) is 1 mm. Figure 6(b) gives the situation when the angle deflection of the first diaphragm in the x direction is 30°. Figure 6(c) gives the situation when the position offset of the second diaphragm in the x direction (positive direction) is 1 mm, and Fig. 6(d) gives the situation when the angle deflection of the second diaphragm in the x direction is 30°.

The figures show that: 1) Compared Fig. 6(a) with Fig. 6(b), the position offset of the first diaphragm can only make output intensity distribution move to the opposite direction of the offset direction of the diaphragm, and the angle deflection of the first diaphragm can create output light beams compression in the same direction of the angle deflection direction of the diaphragm; 2) Compared Fig. 6(c) with Fig. 6(d), the position offset of the second diaphragm make output light distribution covered in the opposite direction of the offset direction of the diaphragm, and the angle deflection of the second diaphragm can also create output light beams compression in the same direction of the angle deflection direction of the diaphragm; 3) Compared Fig. 6(b) with Fig. 6(d), when the angle deflection value is the same, the output light beams compression of the influence of the first diaphragm is more obvious than that of the second diaphragm. In Fig. 6(d), the elliptical diffraction figure is clearly shown in the centre, but the peripheral diffraction light distribution is not clear.

Figure 7 gives the output intensity distribution when both of the diaphragms are disadjust: Figure 7(a) is the situation when the position offsets of the two diaphragms are both 1 mm in the x direction, and Fig. 7(b) is the situation when the angle deflection of the two the diaphragms are both 30° in the x direction. Compared Fig. 7(a) with Figs. 6(a) and 6(c), it could be seen that the output intensity distribution in Fig. 7(a) is the superposition of that in Figs. 6(a) and 6(c), and it is determined by the light's principle of superposition. Compared Fig. 7(b) with Figs. 6(b) and 6(d), the same conclusion can be obtained.

Figure 8 gives the output intensity distribution when only one of the lenses is disadjust: Figure 8(a) gives the situation when the position offset of the first lens in the x direction (positive direction) is 1 mm, and Fig. 8(b) gives the situation when the angle deflection of the first lens in the x direction is 1°; Fig. 8(c) gives the situation when the position offset of the second lens in the x direction (positive direction) is 1 mm, and Fig. 8(d) gives the

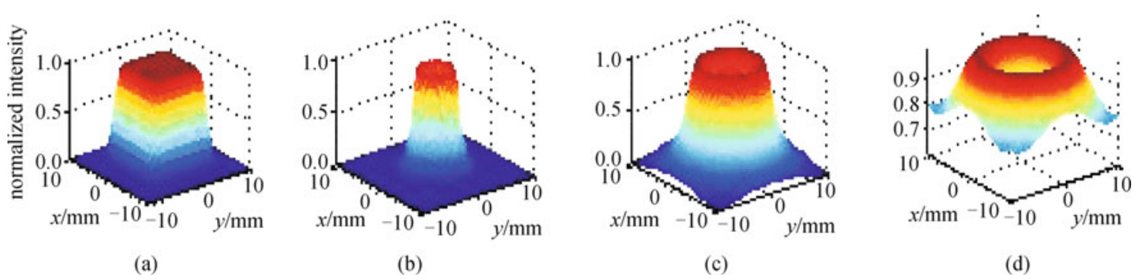

Fig. 4 Normalized intensity distribution in different propagating distances of flat-topped multi-Gaussian beams in normal situation. (a) Initial light beam; (b) $z_3 = 1000$ mm; (c) $z_3 = 2000$ mm; (d) $z_3 = 10000$ mm

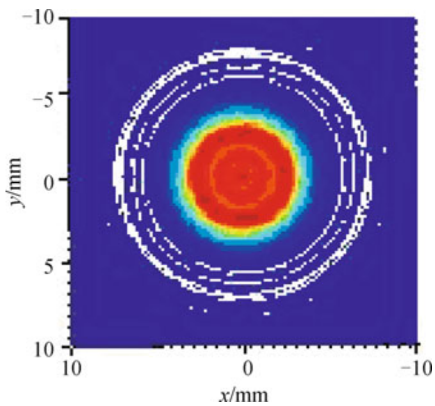

Fig. 5 Output intensity distribution in normal situation

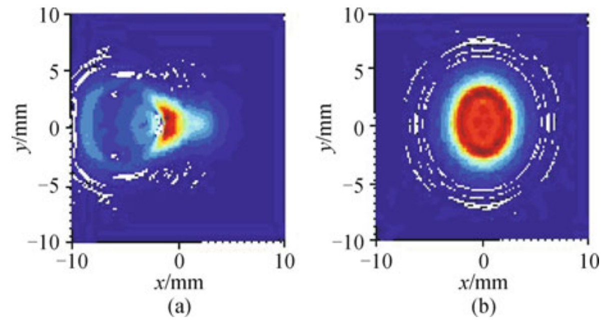

Fig. 7 Output intensity distribution when both of the diaphragms are disadjust. (a) $d_{x1} = d_{x2} = 1$ mm; (b) $\alpha_{x1} = \alpha_{x2} = 30°$

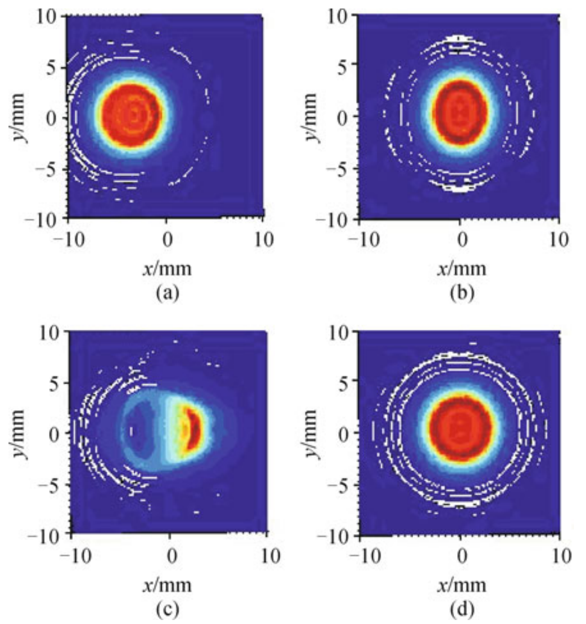

Fig. 6 Output intensity distribution when one of the diaphragms is disadjust. (a) $d_{x1} = 1$ mm; (b) $\alpha_{x1} = 30°$; (c) $d_{x2} = 1$ mm; (d) $\alpha_{x2} = 30°$

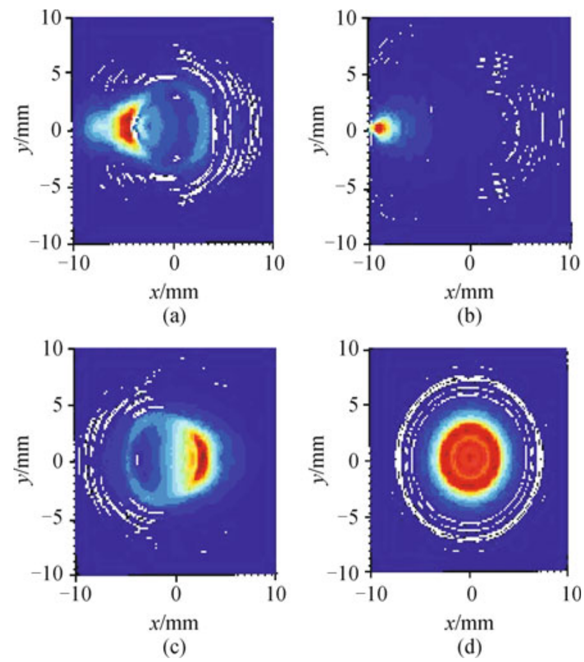

Fig. 8 Output intensity distribution when just one lens is disadjust. (a) $\varepsilon_{x1} = 1$ mm; (b) $\varepsilon'_{x1} = 1°$; (c) $\varepsilon_{x2} = 1$ mm; (d) $\varepsilon'_{x2} = 1°$

situation when the angle deflection of the second lens in the x direction is 1°. Figure 8(a) shows that the offset of the first lens can weaken light intensity in the same direction of the offset direction of the lens, makes diffraction stronger, and makes light beams elongating in the opposite direction of the offset direction of the lens; Fig. 8(b) shows that the angle deflection of the first lens can make light beams move to the opposite direction of the angle deflection direction of the lens; Fig. 8(c) shows that the offset of the second lens can weaken light intensity in the opposite direction of the offset direction of the lens; Fig. 8(d) shows that the angle deflection of the second lens have no influence to output light beams, which can also be seen clearly in Eq. (11).

Figure 9 gives the output intensity distribution when both of the lenses are disadjust. Figure 9(a) gives the situation that the position offsets of the two lenses in the x direction (positive direction) are both 1 mm, and Fig. 9(b) gives the situation when the angle deflection of the two lenses in the x direction are both 1°. Figure 9(a) shows that when both of the lenses exist offsets, the light beams move to the direction of the offset of the second lens, the light beams are stretched in the disalignment direction, and the light beams in the opposite direction of the offset direction of the lens pass through the optical system; Fig. 9(b) shows that the angle deflection of the lenses influences more to the offset of the beam, but the angle deflection of the second lens have no influence on beam transformation.

Figure 10 gives the output intensity distribution when all the diaphragms and lenses are disadjust: the offset of each

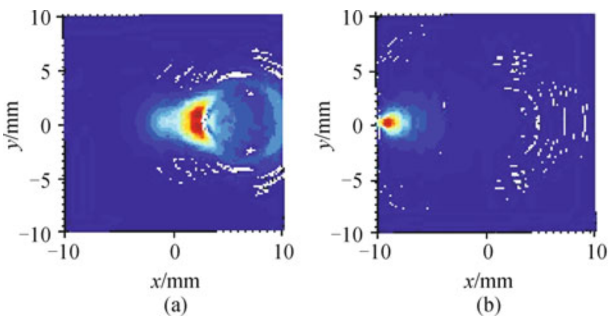

Fig. 9 Output intensity distribution when both lenses are disadjust. (a) $\varepsilon_{x1} = \varepsilon_{x2} = 1$ mm; (b) $\varepsilon'_{x1} = \varepsilon'_{x2} = 1°$

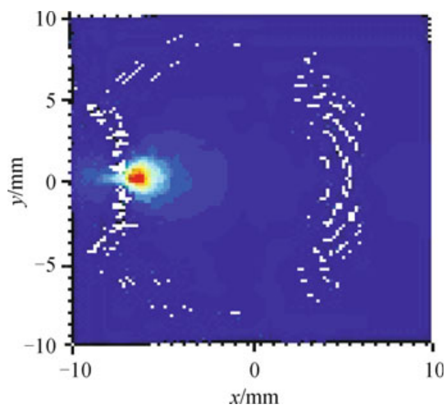

Fig. 10 Output intensity distribution when all lenses and diaphragms are disadjust ($d_{x1} = d_{x2} = \varepsilon_{x1} = \varepsilon_{x2} = 1$ mm, $\alpha_{x1} = \alpha_{x2} = 30°$, $\varepsilon'_{x1} = \varepsilon'_{x2} = 1°$)

diaphragm in the x direction is 1 mm, the angle deflection of each diaphragm in the x direction is 30°, and the offset and angle deflection of each lens are the same. Figure 10 is similar to Fig. 9, thus when all the diaphragms and lenses are disadjust, the angle deflection of lenses has the greatest impact on incident light, and it creates deviation of light beams directly.

5 Conclusion

By using generalized Huygens-Fresnel diffraction formula and approximate expansion of circle diaphragm, a universal analytic expression is deduced approximately for the flat-topped multi-Gaussian beams passing through a misaligned optical system with two-lens and two-diaphragm. Moreover, the method of the complex Gaussian expansion of the aperture function is applicable to the far-zone. In the situations of normal and maladjustment, the propagating property of flat-topped multi-Gaussian beams, which pass through the optical system mentioned above, is studied. The influence of disadjust parameters on output light distribution is analyzed numerically. The result has instructional value for the study in the field of laser-beam propagating and transforming in proper optical systems.

Acknowledgements One of the authors, Shen H. B., would like to thank Dr. Shen X. for his help in this work.

References

1. Wen J J, Breazeale M A. A diffraction beam field expressed as the superposition of Gaussian beams. Journal of the Acoustical Society of America, 1988, 83(5): 1752–1756
2. Ding D, Liu X. Approximate description for Bessel, Bessel-Gauss, and Gaussian beams with finite aperture. Journal of the Optical Society of America A, 1999, 16(6): 1286–1293
3. Lu B, Luo S. Approximate propagation equations of flattened Gaussian beams passing through a paraxial *ABCD* system with hard-edge aperture. Journal of Modern Optics, 2001, 48(15): 2169–2178
4. Jiang H L, Zhao D M, Mei Z R. Propagation characteristics of the rectangular flattened Gaussian beams through circular apertured and misaligned optical systems. Optics Communications, 2006, 260(1): 1–7
5. Chen J N. Propagation and transformation of flat-topped multi-Gaussian beams in a general nonsymmetrical apertured double-lens system. Journal of the Optical Society of America A, 2007, 24(1): 84–92
6. Gori F. Flattened Gaussian beams. Optics Communications, 1994, 107(5–6): 335–341
7. Tovar A A. Propagation of flat-topped multi-Gaussian laser beams. Journal of the Optical Society of America A, 2001, 18(8): 1897–1904
8. Bagini V, Borghi R, Gori F, Pacileo A M, Santarsiero M, Ambrosini D, Spagnolo G S. Propagation of axially symmetric flattened Gaussian beams. Journal of the Optical Society of America A, 1996, 13(7): 1385–1394
9. Cai Y, Lin Q. Light beams with elliptical flat-topped profiles. Journal of Optics A: Pure and Applied Optics, 2004, 6(4): 390–395
10. Cai Y, Lin Q. Properties of a flattened Gaussian beam in the fractional Fourier transform plane. Journal of Optics A: Pure and Applied Optics, 2003, 5(3): 272–275
11. Cai Y, He S. Partially coherent flattened Gaussian beam and its paraxial propagation properties. Journal of the Optical Society of America A, 2006, 23(10): 2623–2628
12. Eyyuboglu H T. Propagation of Hermite-cosh-Gaussian laser beams in turbulent atmosphere. Optics Communications, 2005, 245(1–6): 37–47
13. Cai Y, He S. Propagation of various dark hollow beams in a turbulent atmosphere. Optics Express, 2006, 14(4): 1353–1367
14. Cai Y. Propagation of various flat-topped beams in a turbulent atmosphere. Journal of Optics A: Pure and Applied Optics, 2006, 8 (6): 537–545
15. Eyyuboglu H T, Arpali C, Baykal Y. Flat topped beams and their characteristics in turbulent media. Optics Express, 2006, 14(10): 4196–4207

16. Chu X, Ni Y, Zhou G. Propagation analysis of flattened circular Gaussian beams with a circular aperture in turbulent atmosphere. Optics Communications, 2007, 274(2): 274–280
17. Amarande S A. Beam propagation factor and the kurtosis parameter of flattened Gaussian beams. Optics Communications, 1996, 129(5–6): 311–317
18. Borghi R, Santarsiero M, Vicalvi S. Focal shift of focused flat-topped beams. Optics Communications, 1998, 154(5–6): 243–248
19. Li Y. Light beams with flat-topped profiles. Optics Letters, 2002, 27 (12): 1007–1009